Quaternary Science Reviews 145 (2016) 82–93

Contents lists available at ScienceDirect

Quaternary Science Reviews

journal homepage: www.elsevier.com/locate/quascirev

Timing of wet episodes in Atacama Desert over the last 15 ka. The Groundwater Discharge Deposits (GWD) from Domeyko Range at 25°S.

Alberto Sáez [a, *], Linda V. Godfrey [b], Christian Herrera [c], Guillermo Chong [c], Juan J. Pueyo [d]

[a] Department of Earth and Ocean Dynamics, Facultat de Geologia, Universitat de Barcelona, Marti Franqués s/n, 08028, Barcelona, Spain
[b] Earth and Planetary Sciences, Rutgers University, 610 Taylor Road, Piscataway, NJ 08854, USA
[c] Departamento de Ciencias Geológicas, Universidad Católica del Norte, Avenida Angamos, 0610, Antofagasta, Chile
[d] Facultat de Geologia, Universitat de Barcelona, Marti Franqués s/n, 08028, Barcelona, Spain

ARTICLE INFO

Article history:
Received 25 January 2016
Received in revised form
23 May 2016
Accepted 24 May 2016

Keywords:
Central Andes
Holocene
Pluvial events
Groundwader Discharge Deposits
Wetlands
Summer monsoons

ABSTRACT

A chronologically robust reconstruction of timing and dynamics of millennial time scale wet episodes encompassing the entire Atacama Desert during the last 15 ka has been constructed. To accomplish this, a new composite paleoclimatic record from Groundwater Discharge Deposits (GWD) in the Sierra de Varas (Domeyko Range, southern Atacama in Chile at 25°S) has been compiled and compared with other published paleohydrologic records from the Atacama region. In Sierra de Varas (SV), three millennial timescale wet climate phases have been characterized: around 14.5 ka cal BP, 12.2–9.8 ka cal BP, and 4.7 ka cal BP to the present day. These wet phases are interpreted from intervals of GWD facies formed during periods when the springs were active. GWD facies include: (1) black organic peat, rooted mudstones and sandstones formed in local wetland environments, and (2) gypsum-carbonate rich layers formed by interstitial growth. GWD intervals alternate with gravelly alluvial material deposited during arid phases. A trend towards less humid conditions during the Late Holocene wet episode characterizes GWD sedimentary series in Sierra the Varas, suggesting the onset of a dry episode over the last few centuries. Around 0.7 ka BP a very short wet episode is recorded in the central part of the desert suggesting this was the time of maximum humidity for the entire late Holocene wet period. A brief arid phase occurred between 1.5 and 2.0 ka BP indicated by the absence of GWD in the Domeyko Range. The paleoclimatic reconstruction encompassing the entire Atacama region shows that both the intensity and occurrence of wetter conditions were governed mainly by the distance to the source of moisture, and secondarily by the elevation of the sites. In the northern Atacama (16–20°S), four wet phases fed by N-NE summer monsoon precipitations have been proposed: Tauca phase (18–14 ka cal BP) and Coipasa phase (13–10 ka cal BP) during the Late Glacial, followed by Early Holocene and Late Holocene phases. In contrast, southern Atacama records (23–28°S) display only three pluvial periods which result from SE summer monsoon precipitation and outbreaks from the Westerlies during wintertime. The Early Holocene in the southern Atacama was a period of aridity, generating important landscape differences to those in the Northern Atacama where conditions were wetter. The core of Atacama (20–23°S) is the overall driest part of the desert because it is located in the distal limits of both N-NE and SE sources of moisture, the Amazon Basin and Gran Chaco areas, respectively.

1. Introduction

The Atacama Desert has been one of the driest regions in the world over the last 15 Ma (Hartley and Chong, 2002). This aridity, which is most extreme between the western Andean slope and the coast between ca. 18°S and 26°S has been attributed to: (1) the barrier to Atlantic moisture fluxes provided by the Andes; (2) the inhibition of Pacific moisture by cold water transported by the Humboldt Current that modulates the strength of the subtropical anticyclone and creates a temperature inversion along the coast;

* Corresponding author.
E-mail address: a.saez@ub.edu (A. Sáez).

http://dx.doi.org/10.1016/j.quascirev.2016.05.036
0277-3791/

and (3) its location beyond the northern limit of the Southern Westerlies circulation zone in Norte Chico (Garreaud et al., 2010).

Despite the overall hyperarid conditions, regular precipitation on the western flank of the Andean Range and infrequent precipitation in the Coastal Range occur at the present, as well as in the past, forming a marked alternation between dry and wet periods on millennial time-scales. Studying deposits formed during these wet periods is a first step towards assessing water runoff and replenishment of groundwater reserves (Houston and Hart, 2004; Herrera and Custodio, 2014). These pluvial events were also vital to human subsistence following the initial occupation of the region between 11.5 and 13 ka ago (Moreno et al., 2009; Santoro et al., 2011; Gayó et al., 2015) as well as the last two centuries when water needs for mining, agriculture and human consumption have greatly increased.

A number of paleoclimate reconstructions of pluvial phases over the Cenozoic (Hartley and Chong, 2002; Hartley, 2003; Sáez et al., 1999, 2012; Jordan et al., 2014; de Wet et al., 2015 among others) and Late Quaternary (Rech et al., 2002; Latorre et al., 2006; Nester et al., 2007; Moreno et al., 2007; Quade et al., 2008; Placzek et al., 2009; among others) have been undertaken in the region. Unfortunately, there is a lack of reliable, long and continuous reconstructions to understand the variability in time and space of the climate modes acting in the entire Atacama region. The resulting uncertainties and discrepancies about the timing of wet and dry episodes and the moisture origin hamper the complexities of the regional-scale hydrological cycle from being resolved.

In this study, a paleohydrological and paleoclimate reconstruction on a millennial timescale in the southern part of the Atacama Desert over last 15 ka is presented. The composite reconstruction is based on the sedimentology, mineralogy, geochemistry and chronology of five records of groundwater discharge deposits (GWD) on the western side of the Sierra de Varas, a segment of the Domeyko Range in the western Andean Pre-Cordillera slope (Fig. 1). Because of its hydrological characteristics, the study of GWD records eludes the uncertainty derived from paleoclimate interpretations of lacustrine sediment sequences in the Central Andes owing to the greater water reservoir effect and changes in the effective moisture (precipitation minus evaporation). Comparing these new records to published information of palaeohydrology for the Atacama and its margins, we also reconstruct a north-south transect through the region of wet phases during the last 15 ka at elevations ranging from 1000 to 4500 m.a.s.l. Our understanding of the meteorological mechanisms presently acting in the region allows this reconstruction to address the timing and dynamics of wet periods to propose new arguments regarding unresolved paleoclimatic questions such as: the effect of the elevation in the duration and occurrence of the recorded wet episodes, the potential for groundwater recharge during wet and dry episodes (such as the controversial mid-Holocene arid phase), and landscape differences between the northern and southern parts of the desert.

2. Geological and climatological setting of the study area

The five studied sites (locally described as “aguadas”) are located between 24.5 and 25.2°S, at elevations ranging from 2560 to 3830 m.a.s.l. on the west side of Sierra de Varas (AV, SA, CH, CA, ES) (Fig. 1). Sites are at active water springs, except for SA where pipes installed by nitrate mines almost 100 years ago alter the natural flow. The existence and location of these springs is primarily controlled by geological structures, with more permeable units juxtaposing less permeable bedrock or finer grained sedimentary units, forcing groundwater to the surface (Fig. 2). The five studied sequences record meters-thick successions in which (1) Quaternary alluvial deposits dominated by gravelly sediments alternate with (2) groundwater discharge deposits (GWD, defined by Pigati et al., 2014) as being composed of black organic-rich layers and rooted fine clastic layers, or by gypsum–carbonate rich layers (Fig. 3). The area occupied by these deposits (hectares to tens of hectares) is located some hundreds of meters immediately downstream of an active spring. Deposits, including organic layers, are tilted a few degrees to the west following the modern alluvial fan system surfaces of the western side of Sierra de Varas. A number of trenches (Fig. 4A), some up to 5 m deep, made recently for water extraction by the mining industry, allow the complete exposure of sedimentary sequences related to groundwater discharge episodes. Main compositional differences between these records (Fig. 3, Table 1S) relate to the presence or absence of sulphate and carbonate layers depending on the catchment geology.

The lag time for GWDs to respond to changes in precipitation is not long. Initial studies using cosmogenic nuclides reveal that the tritium level in springs CH, CA and ES is between 2 and 4 times background values, and water that accumulates at a collection point just above the SA sampling location contains more than 5 times the background (Gamboa et al., in prep). Although spring flow under the current climate state does not show measureable intra-annual or inter-annual variability, the presence of tritium indicates that the lack of variability in flow reflects the high evaporation potential for any rain, and sublimation of snow leading to limited and slow infiltration of water through a thick unsaturated zone, rather than leakage from a stagnant groundwater reservoir. The geometry of the Aguada Alto de Varas (AV) spring system differs from the others by a normal fault providing a barrier between the alluvial deposits of the Pampa de Mulas Fm and impermeable Qda. El Salitre volcanics, forming a small high elevation water basin which outflows at the spring. However, since all other springs within the Sierra de Varas, and particularly at the elevation of AV, contain appreciable tritium, the water table of the aquifer reservoir which feeds AV is more likely to fluctuate on a decadal and not multi-centennial scale, even though the size of the water reservoir dilutes any tritium signature of recent infiltration to levels below the detection limit.

Regular precipitation of rain and snow in the Atacama Desert are currently triggered by two modes that control austral summer (rainy season from December to February) monsoonal precipitation in the region between 20 and 30° S that are not in phase (Vuille and Keimig, 2004; Quade et al., 2008). These include (1) moisture originating from Southeastern South America and carried by SE trade winds (SE mode); and (2) precipitation derived from the Atlantic Ocean moisture crossing the Amazonia, and carried by NE trade winds (N–NE mode). Moreover, snow accumulates on the west side of the high Andes of Northern Chile when moisture from the equatorial Pacific is entrained into convective storms during winter-spring (Vuille and Ammann, 1997). During these events, heavy convective rains on the coast of northern Chile and southern Perú (Ortlieb, 1995; Vargas et al., 2000; Jordan et al., 2015) produce debris flow deposits in alluvial fans, broadly recorded during the second half of the Holocene (Vargas et al., 2006). These episodic rains (snow in highlands) have been directly related with the modern high frequency ENSO through weakening of the South Eastern Pacific Subtropical Anticyclone.

Temporal variability in this climate pattern over the Atacama region, led to the suggestion that during the end of the Pleistocene and Holocene, the SE and N-NE climate modes of precipitation must have changed both their absolute and relative intensity on millennial scales, so that the Atacama region experienced relatively wet periods with fewer periods of aridity (Placzek et al., 2009; Quade et al., 2008). These changes have been mainly linked to ENSO variability and changes in the moisture level in the eastern lowlands of Amazonia and the Gran Chaco region of Argentina

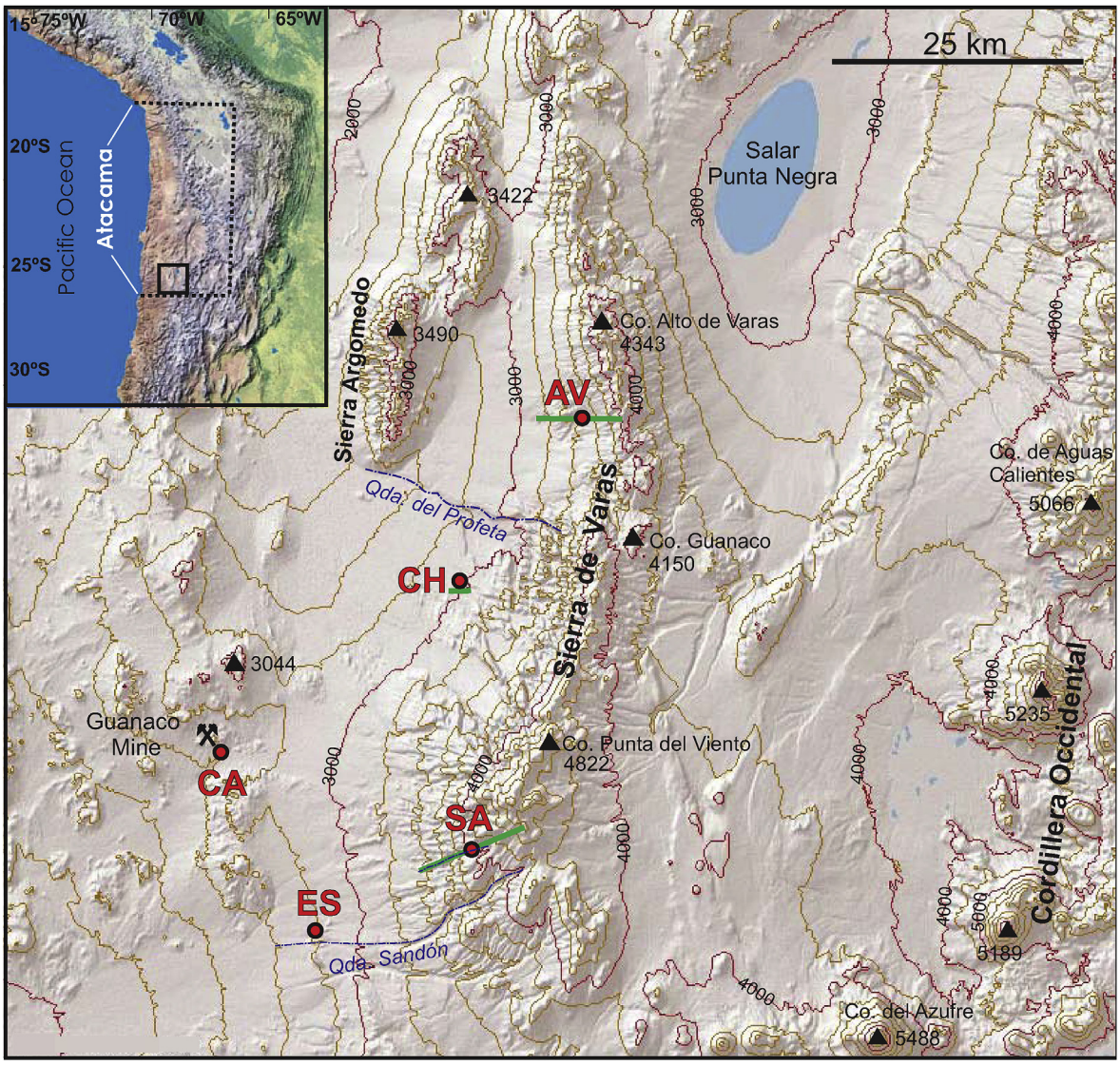

Fig. 1. Topographic map showing location of Groundwater Discharge Deposits in Sierra de Varas sector of the Domeyko Range (*aguadas* of AV Alto de Varas, CH Chepica, CA Cachinalito, SA Quebrada Los Sapos, ES Escondida). Green lines indicate location of cross sections of Fig. 2. (For interpretation of the references to colour in this figure legend, the reader is referred to the web version of this article.)

(Placzek et al., 2009).

3. Methodology

3.1. Facies analyses

During a field study carried out in June 2014, five lithological-sedimentological sequences were measured, described and sampled on the western slope of the Domeyko Range between 24 and 26°S (mainly occupying the area of Sierra de Varas). During logging, sequence sampling protocols were developed in the field for mineralogical, geochemical and dating analysis. About 100 smear slides were prepared in the laboratory to first obtain a description of the sediment and then to semi-quantitatively estimate the biogenic, clastic, and authigenic mineral content using a polarizing microscope.

3.2. Mineralogical and geochemical analyses

A total of 101 samples were taken, dried at 60 °C for 24 h and ground cryogenically (after liquid nitrogen immersion) in a ring mill for around 15 s. The loss on ignition values (LOI; at 450 °C) were calculated. X-ray diffractograms were performed in the 4–60° 2θ interval, using a PANalytical X'Pert PRO MPD-DY 3197 X-ray powder diffractometer under the following conditions: Cu Kα radiation (λ = 1.5418 Å), 40 kV, 30 mA, with graphite monochromator. Total organic carbon (TOC), total inorganic carbon (TIC) and total nitrogen (TN) were also determined in 66 selected samples using a Thermo EA 1108 elemental analyzer working in standard mode (helium flow: 120 mL/min; combustion furnace: 1000 °C; chromatographic column oven: 60 °C; 10 mL oxygen loop at 100 kPa).

3.3. Chronological framework

The chronological framework was primarily built from a total of 33 organic-rich sediment samples selected for ^{14}C dating by AMS at Beta Analytics Laboratory (Table 1). The bulk sediment was treated washing the samples with hot hydrochloric acid (HCl) followed by a sodium hydroxide (NaOH) to remove carbonate and also mobile humic acids. In order to remove modern plant remains the fraction smaller than 180 μm was submitted for dating. The collagen fraction was separated from a bone (SA-5). Radiocarbon ages were

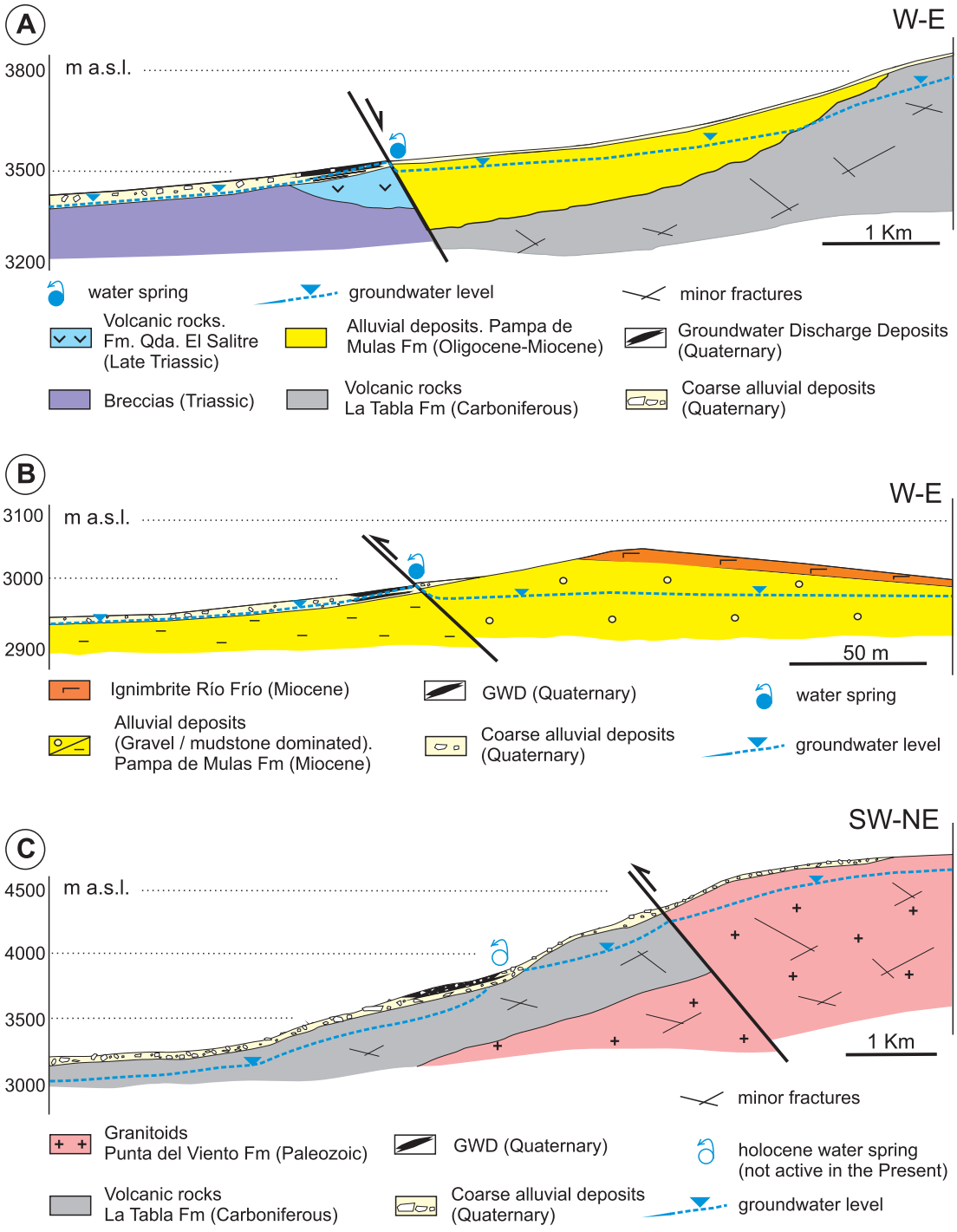

Fig. 2. Cross sections of Alto de Varas (section A), Chepica (section B) and Quebrada Los Sapos (section C). Geological and hydrological elements concerning Groundwater Discharge Deposits formation are represented. Scale of Late Quaternary deposits interbedding GWD are vertically exaggerated. See map of Fig. 1 for cross sections location.

calibrated using CALIB 7.1 (SHCAL13 calibration curve). All ages reported here are given in thousands of calendar years before 1950 (ka). A modern sample (CA-16) was calibrated using the CALIBomb software of Queen's University, Belfast. A carbonate-rich sample (ES-1) was dated by the U/Th series method. Two sample preparation methods were used: (1) discrete grains of gypsum were picked after a sub-sample was disaggregated in an ultrasonic bath followed by complete dissolution; (2) selective dissolution in mineral acids (Table S2). Measurement of $^{230}Th/^{238}U$, $^{234}U/^{238}U$ and $^{232}Th/^{238}U$ were made using the Rutgers University Neptune Plus MC-ICPMS after addition of ^{233}U and ^{229}Th isotope spikes and extraction and separation of U and Th following standard methods (Mortlock et al., 2005).

4. Sierra de Varas groundwater discharge deposits

We describe the facies of sequences involving GWD deposits of the five studied sites, with special emphasis on the Aguada Alto de Varas (AV) site which is the most complete and has the best chronological model. Correlation of lithological units between AV

Table 1
Radiocarbon dates for organic-rich GWD deposits from Sierra de Varas.

No.	Sample id	Laboratory code	Dated material	14C yr BP	$\delta^{13}C$ (‰)	Calibrated age (ka BP)	2 σ (cal. yr BP)
Alto de Varas (AV)		*24°49′11.21″S*	*69°10′42.83″O*	*3446 m a.s.l.*			
1	AVC-20	Beta-384876	Plant	170 ± 30	−28.5	0.13	−79/23
2	AVC-19	Beta-388731	Plant	300 ± 30	−29.9	0.32	−40/15
3	AVC-16	Beta-388730	Plant	880 ± 30	no data	0.74	−59/49
4	AVC-14	Beta-388729	Plant	980 ± 30	no data	0.85	−67/68
5	AVC-12	Beta-388728	Plant	1790 ± 30	−28.5	1.65	−70/74
6	AVC-11	Beta-388727	Plant	1750 ± 30	−30.4	1.62	−66/78
7	AVC-9	Beta-388726	Plant	1700 ± 30	−28.7	1.56	−86/55
8	AVC-7	Beta-388725	Plant	1520 ± 30	−30.0	1.35	−49/55
9	AVC-6	Beta-388724	Plant	2100 ± 30	−27.8	2.03	−46/70
10	AVC-4	Beta-388723	Plant	2560 ± 30	−26.9	2.59	−109/151
11	AVC-3	Beta-384875	Plant	2690 ± 30	−28.4	2.76	−29/78
12	AVC-3[a]	Beta-388823	Organic sediment	2990 ± 30	−28.2	3.10	−115/106
13	AVB-13	Beta-401669	Organic sediment	8860 ± 40	−29.6	9.86	−179/98
14	AVB-9	Beta-384874	Plant	9260 ± 30	−25.6	10.37	−115/122
15	AVB-1[a]	Beta-384873	Plant	8220 ± 40	no data	9.12	−107/144
16	AVB-1	Beta-385822	Organic sediment	10390 ± 40	−24.9	12.20	−205/310
17	AVA-1	Beta-384872	Plant	12450 ± 40	−27.6	14.48	−314/334
18	AVA-1	Beta-385821	Organic sediment	12470 ± 40	−27.5	14.53	−330/253
Chepica (CH)		*24°59′6.80″S*	*69°19′12.32″O*	*2915 m a.s.l.*			
1	CH-10	Beta-384881	Organic sediment	9760 ± 30	−24.3	11.17	−82/57
2	CH-5	Beta-384880	Organic sediment	10330 ± 30	−24.8	12.02	−107/89
Cachinalito (CA)		*25° 8′37.13″S*	*69°33′10.24″O*	*2564 m a.s.l.*			
1	CA -16[a]	Beta-384879	Plant on the surface	210 ± 30	−10.2	0.19	−54/39
2	CA -16[b]	Beta-384879	Plant on the surface	pMC 100.4	modern	AD 1998 CE.7–2000.5	
3	CA-9	Beta-384878	Organic sediment	2030 ± 30	−12.3	1.95	−71/57
4	CA-2	Beta-384877	Charred sediment	9770 ± 30	−22.3	11.18	−84/53
5	CA-2	Beta-385824	Organic sediment	9770 ± 30	−23.8	11.18	−84/53
Quebrada Los Sapos (SA)		*25°12′44.52″S*	*69°17′13.33″O*	*3834 m a.s.l.*			
1	SA-2	Beta-401674	Plant	160 ± 30	−24.8	0.11	−112/41
2	SA-5b	Beta-401673	Bone colagen	270 ± 30	−17.4	0.29	−15/38
3	SA-5a	Beta-401672	Organic sediment	200 ± 30	−24.1	0.19	−52/44
4	SA-5	Beta-401675	Plant	370 ± 30	−23.9	0.39	−77/82
5	SA-9	Beta-401676	Organic sediment	2230 ± 30	−27.0	2.22	−81/90
6	SA-14[a]	Beta-401677	Plant	460 ± 30	−24.1	0.49	−42/31
7	SA-16	Beta-401678	Organic sediment	3080 ± 30	−26.2	3.24	−98/116
8	SA-19	Beta-401679	Organic sediment	3630 ± 30	−25.8	3.89	−69/92
9	SA-21	Beta-401680	Organic sediment	3660 ± 30	−25.7	3.93	−93/67
10	SA-23	Beta-401681	Organic sediment	4170 ± 30	−24.5	4.67	−141/59
Escondida (ES)		*25°17′9.48″S*	*69°26′44.84″O*	*2782 m a.s.l.*			
1	ES-1 (U/Th)	Rutgers Lab.	Carbonates (fine fraction)			2.26	

[a] Not used in age model.
[b] Postbomb calibration.

sequence and the other GWD deposits is represented in Fig. 3 and discussed below.

4.1. Aguada Alto de Varas record

The GWD of Aguada de Alto de Varas (AV, 24°49′11″S, 69°10′43″W, 3446 m.a.s.l.) occupies an area of ca. 32 ha immediately downstream of an active water source which is located 8 km south of the Alto de Varas summit (Fig. 1). Water is forced to the surface at a normal fault where permeable gravel deposits of Pampa de Mulas Fm (Oligocene-Miocene) contact impermeable acid volcanic rocks of Quebrada del Salitre Fm (Late Triassic) (Fig. 2A). A number of trenches excavated into the deposit allowed us to describe and measure a complete composite sequence of GWD sediments (Fig. 4A). The Alto de Varas sequence is 4.9 m-thick and can be divided in four lithological units from the base to the top (Fig. 3).

Unit 1 (12.5–>14.5 ka cal BP)

Unit 1 has a minimum thickness of 3 m and is composed of amalgamated layers of massive-to-poorly stratified, disorganized brown conglomerate and breccia (Facies C). Layers show lenticular shapes and pinch-out laterally in a few meters. Clasts are cobble-to-pebble in size, in a sandy matrix, forming a clast-supported texture. The composition of clasts is dominated by igneous rocks which indicate a provenance from local igneous rocks of Mesozoic – Paleozoic formations. At 60 cm below the top of the unit, a thin black peat layer (Facies A, 32% LOI) is interbedded with the coarse alluvial sediments and has been dated at 14.5 ka cal BP. Facies C depositional features correspond, by comparison to the most recent sedimentation in the area, to lobe alluvial fan deposits. Clasts were transported by debris flows in flashfloods which occurred in the alluvial fan channels during intense rain episodes.

Chronology of the unit is constrained by a single AMS ^{14}C date from the top peat layer (14.5 ka cal BP). Given the virtual absence of organic-rich layers Unit 1 was deposited during relatively dry conditions with a low water-table except for a wet period 14.5 ka cal BP. While the duration of this wet period was short, it is not possible to constrain it because of the lack of similarly aged GWD deposits in the other studied sites.

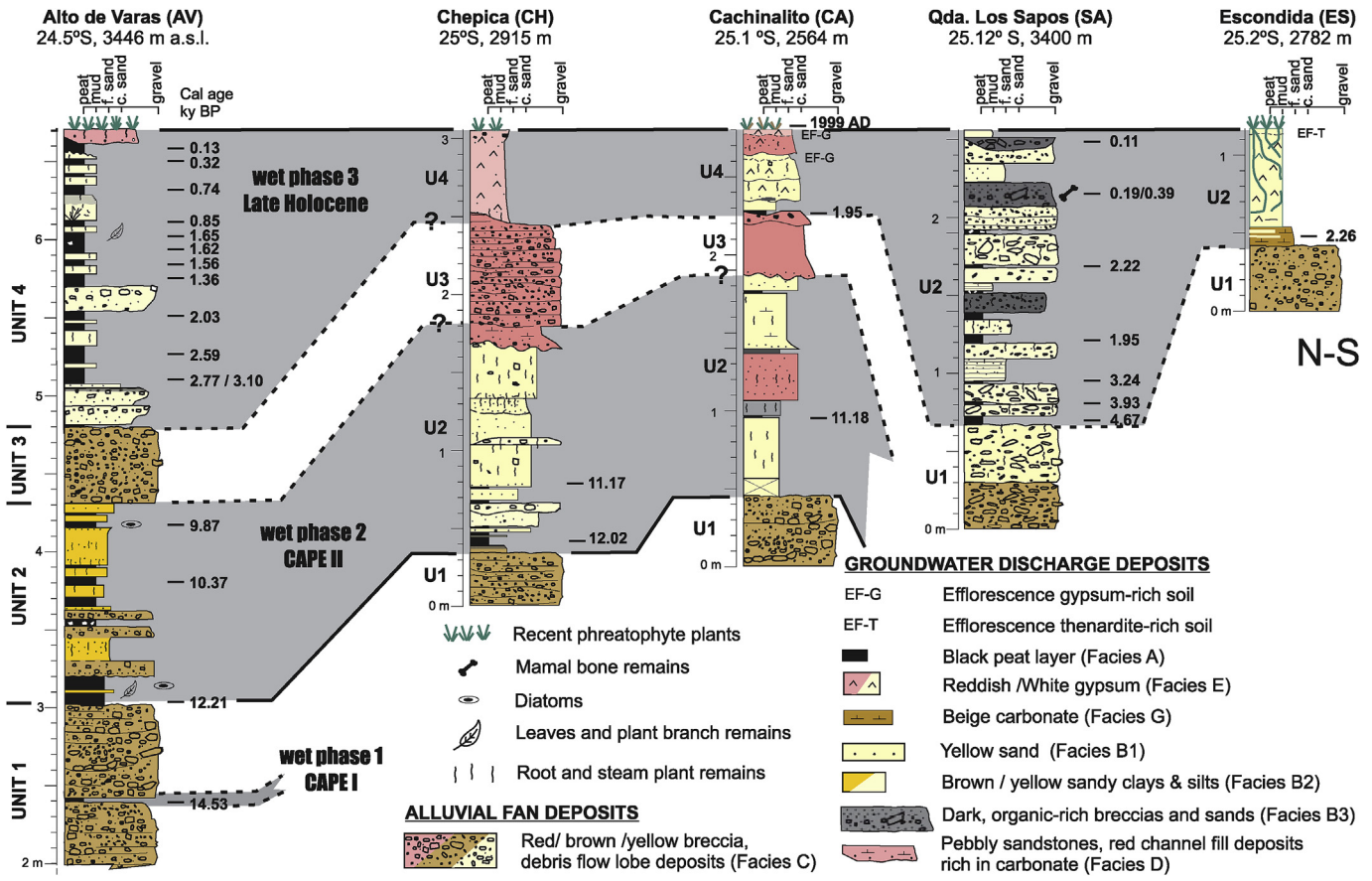

Fig. 3. Correlation panel of studied lithostratigraphic sequences in eastern flank of Sierra de Varas. Coetaneous units of groundwater discharge facies are correlated by a grey pattern indicating wet periods. Facies and facies associations are extensively described in the text.

Unit 2 (12.2–10 ka cal BP)

Unit 2 is 1.24 m-thick and composed of brown mudstones, fine sands and some thin breccia layers. There are up to 8 organic black layers (Facies A). Carbonized root remains which mostly have a vertical orientation are present in all sediments of this unit. Samples from the lower, mid and upper part of the unit yielded ages of 12.2, 10.4 and 9.9 ka cal BP respectively.

Black peat layers (Facies A) are cm-thick, and mainly are composed of plant remains (including leaves and branches) with variable amounts of amorphous organic matter. In addition, phytolites can be very abundant and some layers bear benthic diatom frustules. LOI values range from 12 to 84% in peat-rich samples, but are typically between 50 and 60%. The terrigenous fraction occurs as dispersed siliciclastic sand grains and, in some cases, as pebble lag horizons between organic layers. Significant amounts of scattered diagenetic gypsum crystals (10–25%) and small amounts of ceolites are present in the organic layers. Sands and sandy mudstones (Facies B1 and B2, respectively) are brown, forming cm-to dm-thick slightly erosive layers. Sand particles are mainly composed of variable quantities of quartz (35–50%), plagioclase (25–50%) and K-feldspar (5–15%) whereas the fine mud particles can include significant amounts of muscovite and smectite (Table 1S). Many of the fine-grained terrigenous layers exhibit vertical-carbonized root traces, and have a TOC content up to 5%. Their similar mineralogical distribution indicates a nearby provenance from the small catchments of the alluvial systems. Breccia layers are cm-thick and some are erosive and pinch-out laterally. These coarse facies were deposited by single debris flood episodes and correspond to the C facies described above.

Sedimentological and mapping characteristics of facies associations A and B indicate that they were deposited in wetlands fed by perennial low-energy, stream channelized currents during episodes in which coarse alluvial sedimentation (Facies C) did not occur. This stream-marsh environment (termed “bofedal” or “vega” in Spanish) includes plant and algal mat zones inside and between perennial channels, and occur at several sites of the study area.

In contrast with Unit 1, sedimentological features of Unit 2 indicate a period from 12.2 to 10 ka cal BP of locally wet conditions, where vegetation growth and flow within stream channels was more continuous. Activation of debris flow sediment transport of the alluvial fan system periodically covered and partially eroded the soils and vegetated areas. From the lower part to the top of Unit 2, a thinning upward trend of the peat layers can be recognized, suggesting a gradual transition from relatively wet to less humid climate conditions, culminating with the organic-free sediments of the overlying Unit 3.

Unit 3 (10–>3.1 ka cal BP)

Unit 3 is 0.5 m thick and composed of structureless brown breccias (Facies C), barren of organic-rich sediments. These massive breccia layers represent processes in the alluvial fan channels (both depositional and erosional) during periods when springs were inactive. Considering the ages in the top of Unit 2 and the bottom of Unit 4, the age of this unit could be between 10 and >3.1 ka cal BP. The absence of sedimentation of organic layers in this unit indicate dry conditions during a long period of the mid Holocene, during which the Alto de Varas groundwater sourced springs were inactive or had very reduced activity.

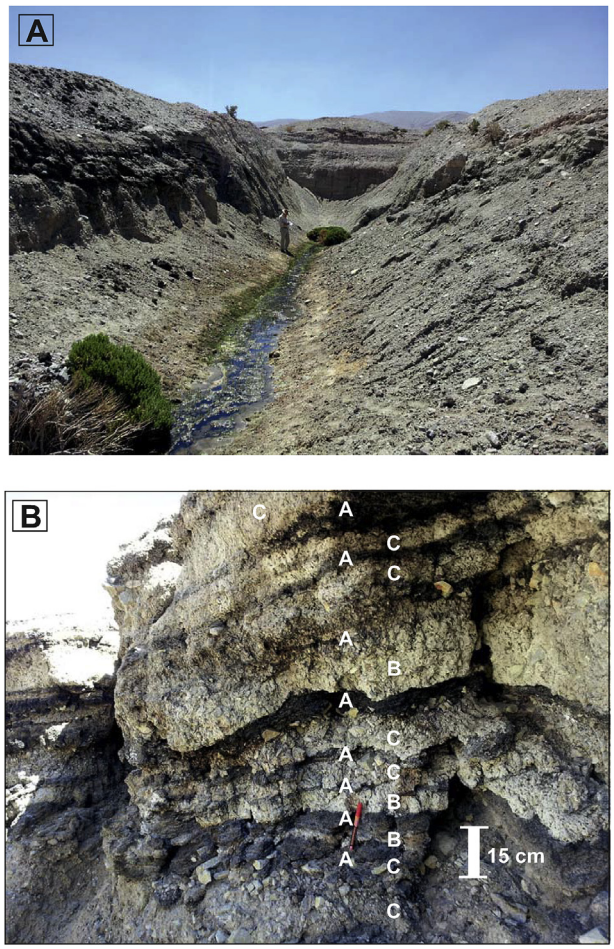

Fig. 4. A. The Aguada Alto de Varas section was done in this trench that was dug to extract water for mining activities in the last decades. The trench cuts the complete sequence of GWD quaternary deposits. B. Upper part (Unit 4) of Aguada Alto de Varas section. An alternation of alluvial deposits (C: Facies C), and groundwater discharge deposits (A: Facies A, B: Facies B) can be recognized.

Unit 4 (>3.1 ka cal BP – present)

Unit 4 is 1.9 m thick and is composed of yellow rooted sands, mudstones, and breccias (Facies B1, B2 and C respectively) which interbed with up to 14 layers of black peat, rich in plant remains and phytoliths (Facies A) (Fig. 4B). In addition, some gravel layers exhibit a dark fine matrix rich in organic matter. The thickness of organic layers does not show any trend. The age of this unit is well constrained by 11 dated radiocarbon layers.

As with Unit 2, the high frequency of organic layers in this unit, which represent 50% of accumulated thickness, points to relatively wet conditions during the Late Holocene at the site. The activity of the groundwater source has continued up to the Present, allowing plant and algal mat zones to develop associated with stream water flow within Aguada Alto de Varas. Nevertheless, a thicker breccia layer interbedded between peat deposits aged 2.0 and 1.4 ka cal BP could indicate a brief dry period.

4.2. Aguada Chépica record

The Groundwater Discharge Deposits of Aguada Chépica (CH, 24°59′7″S, 69°19′13″W, 2915 m a.s.l.) occupy an area of 10 ha and are located 14 km south of the Argomedo Range (Fig. 1). Water is forced to the surface as it encounters a reverse fault within gravels and interbedded mudstones (Pampa de Mulas Fm) which form a barrier to subsurface flow (Fig. 2B). The sequence is 2.70 m-thick and can be divided into four lithological units (Fig. 3).

Unit 1 (>12 ka cal BP)

Unit 1 is composed of basal conglomerate deposits.

Unit 2 (12–>11.2 ka cal BP)

Unit 2 is 1.45 m-thick and is composed of yellow and rooted fine sands and mudstones, (Facies B1 and B2), some thin breccia (Facies C) layers and up to 4 black peat layers (Facies A) in its lower part. The age of the lower part of this unit is 12 to 11.2 ka cal BP. Peaty, organic-rich layers (Facies A) are cm-thick and include small amounts of diagenetic gypsum and zeolites. LOI in these layers is between 10 and 20.5%. Mudstones and sands, which retain root remains, are mainly composed of plagioclase (24–40%), quartz (32–62%) and K-feldspar (6–26%) with small amounts of smectites and muscovite in the muddy layers. At the top, an erosive, muddy sandstone bed rich in carbonate cement (Facies D) points to a transition to the alluvial deposits of Unit 3.

Unit 3

Unit 3 is 0.70 m-thick and is composed of structureless red breccia. These sediments correspond to alluvial deposits. The age of this unit is not constrained. Nevertheless, their stratigraphic position and alluvial features strongly suggest that this unit correlates with the alluvial episode of Unit 3 in the AV sequence.

Unit 4

Unit 4 is 0.5 m-thick and composed of a channelized pinky white gypsum layer with minor amounts of dispersed sand sized siliciclastic grains (Facies E). Gypsum crystals exhibit lenticular morphology (10–20 μm in size) and probably formed as an interstitial growth in a faint organic matrix during a period when enough water was available. The organic matrix was associated with the presence of a mucus composed by cyanobacterial mats and photosynthetic bacteria similar to those found in salinas and playa lakes (Cody, 1979; Thomas and Geisler, 1982). Today these facies now only contain minor amounts of organic remains and pigments which are not datable by ^{14}C AMS. The 'relatively' wet conditions we interpret for this unit match a Late Holocene humid phase contemporaneous with Unit 4 of the AV sequence.

4.3. Aguada Cachinalito record

The Aguada Cachinalito groundwater discharge deposits (CA, 25°8′37″S, 69°33′10″W, 2564 m a.s.l.) occupy an area of 24 ha, 5 km to the south of the Guanaco Mine (Fig. 1). Spring flow is related with the Soledad Fault System that brings impermeable volcanic rocks of Chile-Alemania Fm (Paleocene-Eocene) in contact with the permeable gravels of Pampa de Mulas Fm. The CA sequence is 2.8 m-thick and can be divided in four lithological units from the base to the top (Fig. 3).

Unit 1 (>12 ka cal BP)

Unit 1 has a minimum thickness of 1 m, and is composed of amalgamated layers of massive-to-poorly stratified, disorganized brown conglomerates and breccias (Facies C). This unit can be stratigraphically correlated with Unit 1 of CH and AV sequences.

Unit 2 (around 11.2 ka cal BP)

Unit 2 is 1.25 m-thick and composed of alternating yellow-dominated, rooted sand and mudstones (Facies B1 and B2) which interbed two black-peat organic-rich horizons (Facies A). The lowermost of these horizons has been dated at 11.2 ka cal BP. Both the age and facies of this unit support a correlation with Unit 2

Fig. 5. Map of the Atacama Desert and neighboring areas in the Central Andes region. Paleoclimate records correlated in Fig. 5 and discussed in the text are located.

sediments of AV and CH sequences which also represent deposition during relatively wet conditions.

Unit 3 (>2 ka cal BP)

Unit 3 is 0.75 m-thick, and is composed of erosive, red gravely sandstones (Facies C) corresponding to alluvial-fluvial deposits that accumulated under relatively dry climatic conditions. It is the stratigraphic equivalent to Unit 3 of AV and CH sequences.

Unit 4 (2 ka cal BP to present)

Unit 4 is 0.5 m-thick and composed of pale red gypsiferous, erosive, amalgamated sandstone layers (Facies E). These layers show gypsum rich horizons (around 50%) at the top (Facies EF-G). Gypsum crystals display lenticular habit and formed as interstitial growths in a sandy matrix when there was increased water availability period during wet climatic conditions.

4.4. Aguada Los Sapos record

The Groundwater Discharge Deposits of Aguada Los Sapos (SA, 25°12′45″S, 69°17′13″W, 3834 m a.s.l.) were sampled in a 3 m-deep water well, located in the canyon ("Quebrada" in Spanish) of Los Sapos. This canyon lies within the western side of the highest part of the Sierra de Varas (Fig. 1). Groundwater flows through fractures in the Punta del Viento Paleozoic granitoids and the volcanic rocks of La Tabla Fm (Carboniferous) and creates a GWD in the canyon floor (Fig. 2C).

Above the basal alluvial gravels (Unit 1), a 1.75 cm-thick interval (Unit 2) is composed of GWD deposits in alternation with some thin breccia layers (Facies C). The GWD facies association includes 8 black peat layers (Facies A), yellow mudstones with carbonized roots (Facies B1) and two dark, organic-rich channelized breccia layers that pass laterally to dominant peat (Facies B3). The upper organic-rich breccia layer (sample SA-05b) includes some large mammal bone remains. The dominant GWD facies of Unit 2 defines a wet period during the last 4.7 ka cal BP that encompasses and enlarges the duration of all other wet periods of the Late Holocene recorded in Sierra de Varas. From the lower part to the top of Unit 2, there is a thinning upwards of peat layers pointing to a gradual change from relatively wet to less humid climate conditions.

4.5. Aguada Escondida record

The Groundwater Discharge Deposits of Aguada Escondida (ES, 25°17′10″S, 69°26′45″W, 2782 m a.s.l.) occupy an area of 3 ha that is located 23 km to the SE of the Guanaco Mining District (Fig. 1). Above the basal gravel alluvial deposits (Unit 1), is a 0.75 cm-thick interval (Unit 2) composed of beige carbonate, followed by a white gypsum layer (Facies E) which is capped by a cm-thick efflorescent crust of thenardite (Facies EF-T) (Fig. 3). The carbonate interval is composed of microcrystalline aggregates (Facies G) which have been precipitated from interstitial waters rich in dissolved inorganic carbon (DIC) probably originating from the El Profeta Fm (Upper Triassic- Upper Jurassic) that outcrops widely in the Sierra de Varas. GWD deposits of Unit 2 represent a cycle which is becoming increasingly evaporative.

The beige carbonate layer in this unit was dated using $^{230}Th/^{238}U$, $^{234}U/^{238}U$ and $^{232}U/^{238}U$ plots (Osmond et al., 1970; Ludwig, 2001) at 1.3 ± 1 ka cal BP. Exclusion of data from coarse grained gypsum which formed later, possibly around 1 ka cal BP, increases the carbonate age to 2.26 ± 1 ka cal BP (Table 1 and Table S2). This indicates that carbonate was precipitated during a wet episode in the Escondida spring area at the same time the other four sites recorded a wet interval. As the climate has become more dry, carbonate has been replaced by gypsum.

5. Discussion

5.1. Paleoclimatic significance of Sierra de Varas groundwater discharge records in the southern and central Atacama Desert

The sedimentological and chronological data from groundwater discharge deposits (GWD) in the Sierra de Varas, which are particularly well constrained chronologically in AV sequence, indicate the occurrence of 3 millennial-long wet phases during the last 15 ka in this southern part of the Atacama Desert. These occurred: (1) around 14.5 ka cal BP; (2) between 12.2 and 9.8 ka cal BP; and (3) from 4.7 ka cal BP to the present day.

The vertical facies distribution of all sequences of this Late Holocene wet phase suggests a trend to less humid conditions towards the Present. This can be seen by the gradual disappearance or total absence of organic-rich facies A, or a trend from carbonate to gypsum precipitation at ES. There is a short arid event in which the lowland CH and CA sites saw spring inactivity between 1.5 and 2.0 ka cal BP. It is also noteworthy that Unit 3, documented in its entirety at AV, CH, CA but only in its waning stages at SA and ES, indicates conditions more arid than present between ca. 9.8 and 4.6 ka cal. BP. Arid conditions during the late-early/mid-Holocene following the humidity of the early Holocene are also recorded across the Altiplano (Thompson et al., 1998; Baker et al., 2001) and the western Cordillera of the Andes (Rech et al., 2003; Grosjean et al., 2003).

There are significant differences in the thickness and frequency of organic-rich layers (Facies A) between sequences at higher elevation sites (AV, SA) with those at lower elevations (CH, CA, ES). At higher elevations (around 3400 m.a.s.l.) facies A, which forms under wet conditions, is better developed than it is at lower

elevations (around 2700 m.a.s.l.), especially during Late Holocene. This is consistent with the strong increase in precipitation with elevation in the Central Andes (Garreaud et al., 2003; Houston and Hartley, 2003), as well as the Domeyko Range demonstrated by the pollen study of Maldonado et al. (2005) along a similar altitudinal transect from 2670 to 3500 m.a.sl. in Quebrada del Chaco at 25°S, immediately south of the Sierra de Varas.

Based on the dynamics of wet episodes (number and temporal overlap), correlations can be made between wet stages in the Sierra de Varas and wet periods inferred by other authors from a number of southern and central Atacama Desert sites (Fig. 5). These reconstructions are based on geochemical, mineralogical and biological (diatoms, ostracodes and pollen) changes in non-saline lacustrine, GWD, and fluvial terrace sedimentary sequences (see Fig. 6 caption for references and sites). Paleoclimatic records based on vegetation type present in rodent middens (Latorre et al., 2002, 2003, 2006; Maldonado et al., 2005) have not been included in this correlation because of their discontinuous nature and their decadal to sub-decadal scale of information about wet climate intervals (Grosjean and Veit, 2005; Maldonado et al., 2005). Records based on saline sequences (Bobst et al., 2001; Lowenstein et al., 2003) have not been considered for the correlation due to their large chronological uncertainties.

The records selected are located in the Altiplano at elevations between 4100 and 4400 m (Miscanti, Lejía and Negro Francisco), and on the west flank of the Pre-Cordillera Range at elevations between 1000 and 3000 m (Sierra Moreno, Salar de Punta Negra, Fig. 5). The comparison of all these records needs to take into account: (1) reservoir effects on radiocarbon ages which can cause variable (and potentially large) uncertainties on dates; (2) the large increase in precipitation amount with altitude that occurs in the Atacama and that is clearly shown in the Sierra de Varas sequences; (3) the late Holocene wet period which is considered here as a single event when, in fact, it is likely to have a complex structure governed by the recent (last 5 ka) strong ENSO dynamics (Moy et al., 2002; Carré et al., 2012, 2014) with rapid changes in

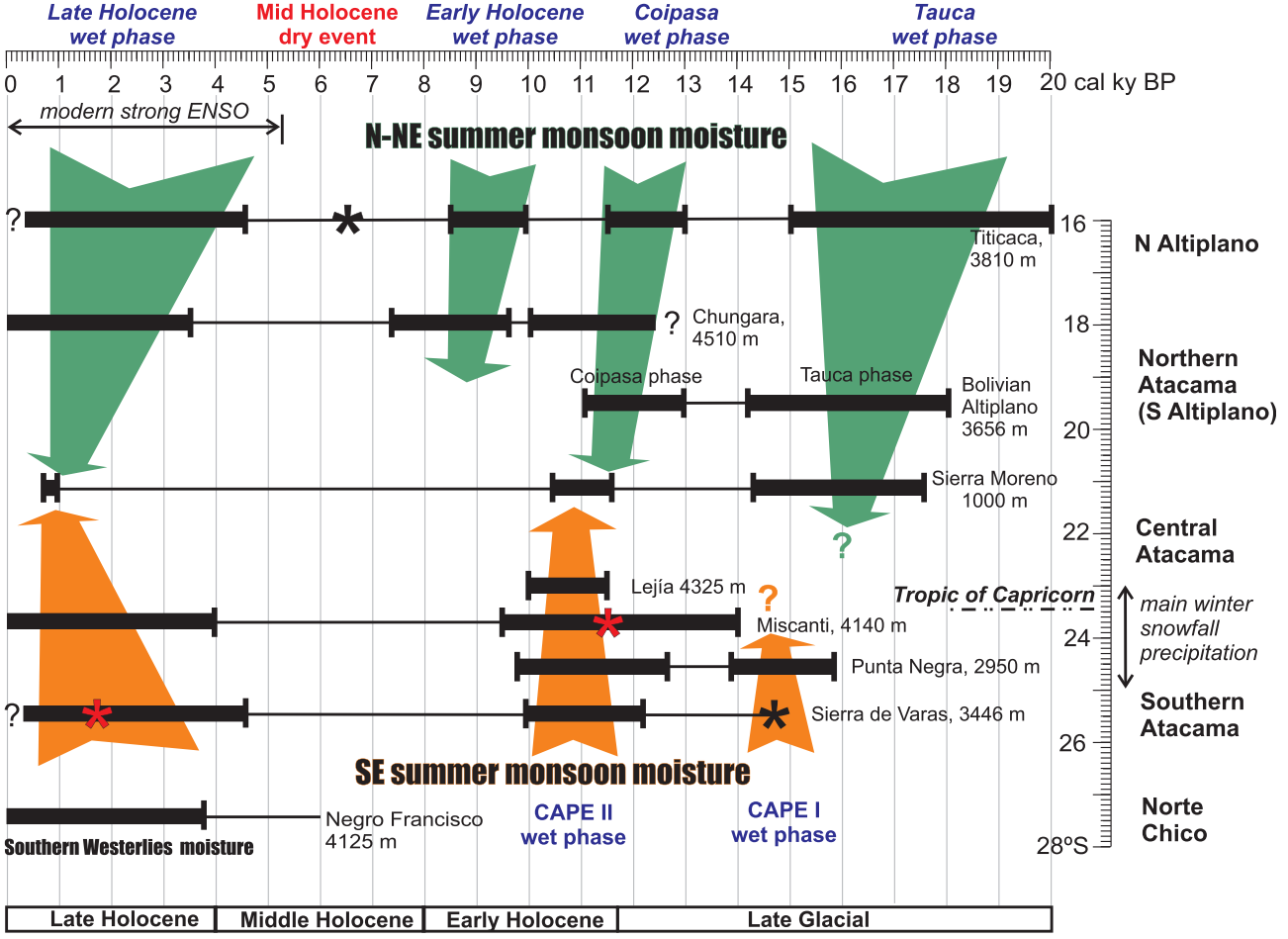

Fig. 6. Compilation of wet events from paleoclimate records done along a transect between 16 and 28°S latitude in the Atacama Desert and neighboring areas over the Late Glacial and Holocene. Thick black segments indicate wet periods and thin lines correspond to relative dry periods. Arrows indicate the main moisture source during wet episodes: green arrows corresponds to Atlantic moisture from the north and northeast crossing the Amazon basin and orange arrows corresponds to moisture from the Gran Chaco region in Argentina. The decrease in width of the arrows indicates the change in the intensity and frequency of precipitations (snow and rain) depending on the proximity from moisture source areas. Black asterisk indicates a wet period dated by only one sample. Red asterisk indicate a short dry period. 1. Lake Titicaca: ostracode, saline diatoms, % freshwater plankton, $\delta^{13}C$ organic, % $CaCO_3$ (Argollo and Mourguiart, 2000; Baker et al., 2001); 2. Chungará Lake: % $CaCO_3$, elemental geochemistry and benthic/planktonic diatoms ratio (Sáez et al., 2007; Moreno et al., 2007; Bao et al., 2015). 3. Lake paleoshoreline deposits in Poopo, Coipasa, Uyuni lakes (Placzek et al., 2006); 4. Organic sediments in fluvial terrace deposits in Quebrada Mani of Sierra Moreno (Nester et al., 2007; Gayó et al., 2012a,b); 5. Laguna Lejía: Mg/Ca and Sr/Ca from sediments (Grosjean et al., 1995; Geyh et al., 1999); 6. Laguna Miscanti: geochemical, mineralogy and facies analysis in sediments and pollen (Grosjean et al., 2001, 2003); 7. Salar de Punta Negra: organic layers in groundwater discharge deposits (Quade et al., 2008); 8. Sierra de Varas (southern Domeyko Range): organic and carbonate layers in groundwater discharge deposits (this work); 9. Negro Francisco Lake (Norte Chico): mineralogy, chemical composition and sedimentary facies analyses (Grosjean et al., 1997). (For interpretation of the references to colour in this figure legend, the reader is referred to the web version of this article.)

precipitation (Valero-Garcés et al., 2003; Latorre et al., 2006; Gayó et al., 2012a); and (4) snowfall during austral winter (May-September) which occurs between 23 and 25 °S by northward displacements or cut-offs of air masses from the Pacific (Vuille and Ammann, 1997).

Within these constraints, the Last Glacial wet interval in the Sierra de Varas corresponds to the so called Central Andean Pluvial Event (CAPE), first named by Latorre et al. (2006) based on a record from the Río Salado in the western Andean flank (22°S between 2910 and 3150 m.a.s.l.) and which has subsequently been split in two wet phases CAPE I (17.5–14.2 ka) and CAPE II (13.8–9.7 ka) (Quade et al., 2008; Placzek et al., 2009). CAPE I and CAPE II wet phases have been recognized as organic-rich layers formed in shallow paleo wetlands in Salar de Punta Negra (Quade et al., 2008) and aggraded terraces of Quebrada Maní in the Sierra Moreno (Nester et al., 2007; Gayó et al., 2012a, 2012b), while CAPE II was recognized, but not well age-constrained, as highstand lake levels in lakes Miscanti (Grosjean et al., 2001, 2003) and Lejía (Grosjean et al., 1995; Geyh et al., 1999). The Late Holocene wet episode, which is well age-constrained in AV and SA sequences in the Sierra de Varas, correlates well with the Late Holocene highstand episodes described in lakes Miscanti (Grosjean et al., 2001, 2003), Negro Francisco (Grosjean et al., 1997), and the fluvial terraces of the Sierra Moreno (Fig. 5). Nevertheless, for the Late Holocene wet episode we need to consider: (1) if less humid conditions, recognized in the Sierra Moreno and CH, CA, ES sequences of the Sierra de Varas over the last couple of centuries, point to the end of this major millennial wet phase, or (2) if it can only be interpreted as a less humid episode within overall wet conditions, and is a product of modern ENSO variability at centennial time scales (Moy et al., 2002; Carré et al., 2012, 2014).

5.2. Northern versus southern Atacama Desert paleohydrology

On millennial time scales, wet phases in the northern Atacama have been identified in a number of records derived from large Altiplano lakes between 3600 and 4500 m.a.s.l. (Titicaca, Chungará, and southern Bolivian lakes). The timing of these wet phases is different to those in the southern Atacama, particularly the occurrence of a wet episode during Early Holocene which is not recorded in the south. Thus, a composite sequence of northern records shows the occurrence of four wet phases (Fig. 6): Tauca phase, Coipasa phase, Early Holocene phase and Late Holocene phase.

The Tauca and Coipasa wet phases were defined by highstand phases in lakes of the southern Altiplano of Bolivia between 18 and 14, and between 13 and 10 ka cal BP respectively (Argollo and Mourguiart, 2000; Placzek et al., 2006). The Tauca phase has also been recognized in Lake Titicaca (Baker et al., 2001), and the Coipasa phase matches the highstand phases in the Titicaca and Chungará lakes (Bao et al., 2015) (Figs. 5 and 6). Early and Late Holocene pluvial episodes are recorded in both Titicaca and Chungará lakes by the same authors, but not in Bolivian Altiplano lakes largely due to the lack of good records.

At this regional scale, the duration in time (and possibly the occurrence) of deposits with sedimentary facies indicating wet climate conditions, is also conditioned by the elevation of the site. The most pronounced differences occur in the late Holocene. While wet periods are recorded over at least the last 3500 years at elevations between 2900 and 4500 m.a.s.l., sites at lower elevations (between 1000 and 2900 m.a.s.l.) only record this period over a few hundred years around 0.75 ka cal BP, suggesting that this was the wettest period of the late Holocene.

5.3. The origin of moisture and timing of wet episodes

The ordering of wet episodes in time and on a North-South transect along the whole Atacama region provides us clues about the moisture source areas that fed summer monsoonal precipitations to different parts of the desert.

Isotope studies of snow records indicate that recent precipitation in the Altiplano highlands of the northern Atacama is principally derived from the tropical Atlantic moisture transported across the Amazon Basin (Thompson et al., 1998; Aravena et al., 1999). This source of moisture also accounts for the pluvial stages during the last glacial period, including the Last Glacial Maximum, as recorded by stable isotopes of brine trapped in halite in the Salar de Atacama (23.5 °S; Godfrey et al., 2003), with the caveat that the lakes which formed in that basin may have been filled by groundwater which recharged further to the east.

The sedimentary record of the central Atacama Desert is key to understanding the extensional limit of moisture provenance between northern and southern Atacama regions. The only long paleoclimate record available in the central Atacama is located in the western flank of Sierra Moreno, 20–23 °S (Figs. 5 and 6). There, three pluvial events have been identified at 17.6–14.2, 12.1–11.4 and 1.01–0.71 cal ka BP (Nester et al., 2007; Gayó et al., 2012a,b). The duration of these pluvial events is shorter than contemporaneous events in the northern and southern Atacama, and is consistent with the overall drier conditions in the core of Atacama Desert. Beyond the effects due to the relative elevation of where these records are derived, the overall shorter duration of pluvial episodes registered in the central Atacama and the apparent absence of the pluvial episode of the early Holocene (Fig. 6), was largely caused by its remoteness from eastern moisture sources. Since the western slope of the Sierra de Moreno receives water mostly from the summit of the Pre-Cordillera, any presumption the lower humidity was a product of the lower elevation of the site would be incorrect.

Considering the timing and frequency of the wet episodes in the central and southern Atacama (except for the CAPE I phase which is not well represented), the records show that humid phases lasted longer in the southern than in the central Atacama (Fig. 6). This pattern is also consistent with modern climate conditions where moisture reaching the southern Atacama comes predominantly from the S-SE and is associated with a monsoonal precipitation mode originating in the Chaco region of Argentina. While this moisture rarely reaches latitudes north of the Tropic of Capricorn today, the CAPE II and late Holocene short wet episodes identified in the Sierra de Moreno could be related to this source area (Fig. 6).

Isotopic data in carbonate lacustrine facies have suggested that moisture coming from the Pacific Ocean influenced the western slopes of the Calama Basin (22.3°S) during the Late Miocene-Pliocene (de Wet et al., 2015). To the south of Atacama, Negro Francisco Lake (28°S) which is located in the transition to the central Chile climatic region shows evidence of receiving mostly moisture from the Pacific carried by the Southern Westerlies during the Late Holocene (Grosjean et al., 1997). While the dominance of N-NE and SE regimes during typical years suggests that these would also be sources of moisture during the Late Quaternary, we cannot rule out that incursions of Pacific moisture, already proven to impact springs in the Coastal Cordillera (Herrera and Custodio, 2014) penetrated further into the core of the Atacama Desert. However, it will be necessary to find and study new continuous paleohydrological records located along West-East transects in key latitudes of the Atacama Desert to understand temporal and spatial patterns associated with Pacific moisture precipitation.

5.4. The mid Holocene and other dry events

In Sierra de Varas, breccia units in the absence of GWD deposits characterizes deposition in alluvial fans during arid periods. The amalgamation of these alluvial coarse and erosive layers of breccia (Facies C) and the relatively low sedimentation rate of the breccia units (Fig. 3) point to a regime with low-frequency storm events. While this regime is overall arid, torrential run-off and flood events triggering debris flows have been associated with discrete events of groundwater recharge in adjacent basins (Grosjean and Veit, 2005).

From the arid periods recorded in Sierra de Varas, our best age constraint for the mid Holocene dry event is between 9.5 and 4 ka BP, which corresponds with mid Holocene arid periods described in southern Atacama records (Grosjean et al., 2001, 2003). In contrast the existence of an early Holocene wet phase recorded in northern Atacama, reduces the duration of the mid Holocene dry event from 7.5 to 4 ka BP.

Dramatic drops in water levels in southern Bolivian Lakes and in their regional water supplies have been recorded during the last few decades (Zolá and Bengtsson, 2006; Arsen et al., 2013) to centuries (Abbott et al., 1997). This apparent arid episode, coupled with current global warming, may contribute to a potential demise of the wet phase during recent times in northern sectors of the Atacama and the Altiplano, and may also be affecting the central and southern Atacama sectors, as the Late Holocene GWD sedimentary trend of Sierra de Varas suggest. However, additional studies of records with higher resolution than we have are necessary to confirm that this recent phase of increasing aridity effectively encompasses all of the Atacama region. They are also required to determine the effects of high frequency variability in ENSO and changes in the phase of the Pacific Decadal Oscillation (PDO) which varies over longer time scales (MacDonald and Case, 2005), but with similar characteristics to ENSO, might amplify its effects if both have the same phase.

5.5. Landscape changes in Atacama during last 14 ka

The reconstruction of the wet (and dry) episodes presented here demonstrates that within the arid region of the Atacama, a boundary between two precipitation regimes (North and South) has been centrally located at least for the last 15 ka. The climate is characterized by alternating wet and dry periods with each lasting thousands of years. Although these wet periods are governed by different atmospheric dynamics, the resulting precipitation regimes have been more or less coupled during the Late Holocene wet phase (last 4.5 ka), Coipasa wet phase (10–12.5 ka) and the Tauca wet phase (14–18 ka), generating a homogeneous landscape across the Atacama for long periods of time. In contrast, during the Early Holocene (8–9.5 ka) the northern part of Atacama had a more vegetated landscape with active springs than would have been found in the central and southern parts of the region. To get a sense of rainfall amounts, vegetation models from Latorre et al. (2002) estimate that during the wet period of the Late Glacial, the primary production was 10–20 times higher than today and that the vegetation covered between 50% and 80% of the land surface, whereas modern vegetation cover is less than 5%.

6. Paleoclimatic conclusions

The Groundwater Discharge Deposits of Sierra de Varas (24–25°S) allow a fairly complete reconstruction of wet episodes at a millennial timescale in this sector of the Domeyko Range in the Atacama Desert during the Late Glacial and Holocene. Wetland sediments were deposited during the pluvial phases: CAPE I (around 14.5 ka cal BP), CAPE II (12.2 and 9.8 ka cal BP) and the wet phase of the Late Holocene (from 4.7 ka cal BP to the present day), with wettest conditions experienced around 0.75 ka BP. This last phase includes a brief return to arid conditions between 2.0 and 1.5 ka BP, and is currently undergoing a trend towards less humid conditions over the last few centuries.

In the northern part of the Atacama, summer monsoon precipitation coming from Amazonia are distributed in 4 wet periods (Tauca phase 18–14 ka cal BP, Coipasa phase 13–10 ka cal BP, Early Holocene and Late Holocene phases). Their area of influence reaches 20°S. In the southern part of Atacama, the monsoon summer precipitation coming from the SE, are distributed in only 3 wet phases (CAPE I, CAPE II and Late Holocene) and extends its influence up to 24°S.

In central Atacama (between 20 and 22°S, close to the Tropic of Capricorn), and distal from both N and S moisture source areas, the short duration of wet periods indicates the driest conditions in the Atacama. This zone received moisture mainly from the N-NE mode during CAPE I and probably from both modes during CAPE II and Late Holocene. Early Holocene humid conditions, recognized in the northern Atacama, did not reach the central or southern sectors of the Atacama.

The compilation of selected sedimentary records shows that the North-South distribution of austral summer precipitation during the last 15 ka was controlled by the intensity variations of the N-NE and S climatic modes that are active at present. Available data do not allow us to assess the secondary role of winter contributions of moisture derived from the Pacific on the interior of Atacama.

The impacts of the high and medium frequency climate phenomena of ENSO and the PDO prevent us from categorically stating that the Late Holocene wet period of the last few centuries is ending, although it is implied from the sedimentary trends recorded in the GWD deposits of the Sierra de Varas.

Acknowledgements

This research was funded by the Anillo project ACT 1203 of the CONICYT of Chile government. We gratefully acknowledge Jerson Escudero for his help in field campaigns and Roberto Bao for interpret diatoms associations. We also thank Rick Mortlock for his help with the U and Th isotope analyses. Comments by two anonymous reviewers helped improve the manuscript.

Appendix A. Supplementary data

Supplementary data related to this article can be found at http://dx.doi.org/10.1016/j.quascirev.2016.05.036.

References

Abbott, M.B., Binford, M.W., Brenner, M., Kelts, K.R., 1997. A 3500 14C yr high-resolution of water-level changes in Lake Titicaca, Bolivia/Peru. Quat. Res. 47, 169–180.

Aravena, R., Suzuki, O., Peña, H., Pollastri, A., Fuenzalida, H., Gilli, A., 1999. Isotopic composition and origin of the precipitation in. North. Chile Appl. Geochem. 14, 411–422.

Argollo, J., Mourguiart, P., 2000. Late Quaternary climate history of the Bolivian Altiplano. Quat. Int. 72, 37–51.

Arsen, A., Crétaux, J.-F., Berge-Nguyen, M., del Rio, R.A., 2013. Remote sensing-derived bathymetry of Lake Poopó. Remote Sens. 6, 407–420.

Baker, P.A., Rigsby, C.A., Seltzer, G.O., Fritz, S.C., Lowenstein, T.K., Bacher, N.P., Veliz, C., 2001. Tropical climate changes at millennial and orbital timescales on the Bolivian Altiplano. Nature 409, 698–701.

Bao, R., Hernández, A., Sáez, A., Giralt, S., Prego, R., Pueyo, J.J., Moreno, A., Valero-Garcés, B.L., 2015. Climatic and lacustrine morphometric controls of diatom paleoproductivity in a tropical andean lake. Quat. Sci. Rev. 129, 96–110.

Bobst, A.L., Lowenstein, T.K., Jordan, T.E., Godfrey, L.V., Hein, M.C., Ku, T.-L., Luo, S., 2001. A 106 ka paleoclimate record from drill core of the Salar de Atacama, northern Chile. Palaeogeogr. Palaeoclimatol. Palaeoecol. 173, 21–42.

Carré, M., Azzoug, M., Bentaleb, I., Chase, B.M., Fontugne, M., Jackson, D., Ledru, M.-P., Maldonado, A., Sachs, J.P., Schauer, A.J., 2012. Mid-Holocene mean climate in

the south eastern Pacific and its influence on South America. Quat. Int. 253, 55–66.
Carré, M., Sachs, J.P., Purca, S., Schauer, A.J., Braconnot, P., Falcón, R.A., Julien, M., Lavallée, D., 2014. Holocene history of ENSO variance and asymmetry in the eastern tropical Pacific. Science 1252220.
Cody, R.D., 1979. Lenticular gypsum: occurrences in nature and experimental determinations of effects of soluble green plant material on its formation. J. Sediment. Pet. 49, 1015–1028.
de Wet, C.B., Godfrey, L., de Wet, A.P., 2015. Sedimentology and stable isotopes from a lacustrine-to-palustrine limestone deposited in an arid setting, climatic and tectonic factors: Miocene-Pliocene Opache Formation, Atacama Desert, Chile. Palaeogeogr. Palaeoclimatol. Palaeoecol. 426, 46–67.
Garreaud, R.D., Vuille, M., Clement, A., 2003. The climate of the Altiplano: observed current conditions and mechanisms of past changes. Palaeogeogr. Palaeoclimatol. Palaeoecol. 194, 5–22.
Garreaud, R.D., Molina, A., Farias, M., 2010. Andean uplift, ocean cooling and Atacama hyperaridity: a climate modeling perspective. Earth Planet. Sci. Lett. 292, 39–50.
Gayó, E.M., Latorre, C., Jordan, T.E., Nester, P.L., Estay, S.A., Ojeda, K.F., Santoro, C.M., 2012a. Late Quaternary hydrological and ecological changes in the hyperarid core of the northern Atacama Desert (~21°S). Earth Sci. Rev. 113, 120–140.
Gayó, E.M., Latorre, C., Santoro, C.M., Maldonado, A., De Pol-Holz, R., 2012b. Hydroclimate variability in the low-elevation Atacama Desert over the last 2500 years. Clim. Past 8, 287–306.
Gayó, E.M., Latorre, C., Santoro, C.M., 2015. Timing of occupation and regional settlement patterns revealed by time-series analyses of an archaeological radiocarbon database for the South-Central Andes (16°-25°S). Quat. Int. 356, 4–14.
Geyh, M.A., Grosjean, M., Núñez, L., Schotterer, U., 1999. Radiocarbon reservoir effect and the timing of the late-Glacial/Early Holocene humid phase in the Atacama Desert (northern Chile). Quat. Res. 52, 143–153.
Godfrey, L.V., Jordan, T., Lowenstein, T.K., Alonso, R.L., 2003. Stable isotope constraints on the transport of water to the Andes between 22° and 26°S during the last glacial cycle. Palaeogeogr. Palaeoclimatol. Palaeoecol. 194, 299–317.
Grosjean, M., Veit, H., 2005. Water resources in the arid mountains of the Atacama Desert (Northern Chile): past climate change and modern conflicts. In: Huber, U.M., Bugmann, H.K.M., Reasoner, M.A. (Eds.), Global Change and Mountain Regions: an Overview of Current Knowledge. Springer, Heidelberg, Germany, p. 650.
Grosjean, M., Geyh, M.A., Messerli, B., Schotterer, U., 1995. Late-glacial and early Holocene lake sediments, groundwater formation and climate in the Atacama Altiplano 22–24°S. J. Paleolimnol. 14, 241–252.
Grosjean, M., Valero-Garcés, B.L., Geyh, M.A., Messerli, B., Schotterer, U., Schreier, H., Kelts, K., 1997. Mid- and late-Holocene limnogeology of Laguna del Negro Francisco, northern Chile, and its palaeoclimatic implications. The Holocene 7, 151–159.
Grosjean, M., van Leeuwen, J.F.N., van der Knaap, W.O., Geyh, M.A., Ammann, B., Tanner, W., Messerli, B., Núñez, L.A., Valero-Garcés, B.L., Veit, H., 2001. A 22,000 14C year BP sediment and pollen record of climate change from Laguna Miscanti (23° S), northern Chile. Glob. Planet. Change 28, 35–51.
Grosjean, M., Cartajena, I., Geyh, M.A., Nuñez, L., 2003. From proxy data to paleoclimate interpretation: the mid-Holocene paradox of the Atacama Desert, northern Chile. Palaeogeogr. Palaeoclimatol. Palaeoecol. 194, 247–258.
Hartley, A.J., 2003. Andean uplift and climate change. J. Geol. Soc. Lond. 160, 7–10.
Hartley, A.J., Chong, G., 2002. Late Pliocene age for the Atacama Desert. implications for the desertification of western South America. Geology 30, 43–46.
Herrera, C., Custodio, E., 2014. Origin of waters from small springs located at the northern coast of Chile, in the vicinity of Antofagasta. Andean Geol. 41, 314–341.
Houston, J., Hart, D., 2004. Theoretical head decay in closed basin aquifers: an insight into fossil groundwater and recharge events in the Andes of northern Chile. Q. J. Eng. Geol. Hydrogeol. 37, 131–139.
Houston, J., Hartley, A.J., 2003. The central Andean west-slope rainshadow and its potential contribution to the origin of hyper-aridity in the Atacama Desert. Int. J. Climatol. 23, 1453–1464.
Jordan, T.E., Kirk-Lawlor, N.E., Blanco, N., Rech, J.A., Cosentino, N.J., 2014. Landscape modification in response to repeated onset of hyperarid paleoclimate states since 14 Ma, Atacama Desert, Chile. GSA Bull. 126, 1016–1046.
Jordan, T.E., Riquelme, R., González, G., Herrerra, C., Godfrey, L., Colucci, S., Gamboa, C., Urrutia, J., Tapia, L., Centella, K., Ramos, H., 2015. Hydrological and geomorphological consequences of the 100 year (?) precipitation event of 24–26 March 2015. In: Published Abstracts XIV Congreso Geologico Chileno, La Serena, Chile.
Latorre, C., Betancourt, J.L., Rylander, K.A., Quade, J., 2002. Vegetation invasions into Absolute Desert: A 45,000-yr rodent midden record from the Calama–Salar de Atacama Basins, northern Chile (22–24uS). Bull. Geol. Soc. Am. 114, 349–366.
Latorre, C., Betancourt, J.L., Rylander, K.A., Quade, J., Matthei, O., 2003. A vegetation history from the arid prepuna of northern Chile (22-23° S) over the last 13,500 years. Palaeogeogr. Palaeoclimatol. Palaeoecol. 194, 223–246.
Latorre, C., Betancourt, J.L., Arroyo, M.K.T., 2006. Late Quaternary vegetation and climate history of a perennial river canyon in the Río Salado basin (22°S) of Northern Chile. Quat. Res. 65, 450–466.
Lowenstein, T.K., Hein, M.C., Bobst, A.L., Jordan, T.E., Ku, T.L., Luo, S., 2003. An assessment of stratigraphic completeness in climate-sensitive closed-basin lake sediments: Salar de Atacama. Chile. J. Sediment. Res. 73, 91–104.
Ludwig, K., 2001. Isoplot/Ex, Rev. 2.49: A geochronological toolkit for Microsoft Excel. In: Spec. Publ. 1a, Berkeley Geochronology Center, Berkeley, California.
MacDonald, G.M., Case, R.A., 2005. Variations in the Pacific Decadal Oscillation over the past millennium. Geophys. Res. Lett. 32 http://dx.doi.org/10.1029/2005GL022478.
Maldonado, A., Betancourt, J.L., Latorre, C., Villagrán, C., 2005. Pollen analyses from a 50000-yr rodent midden series in the southern Atacama Desert (25°30′S). J. Quat. Sci. 20, 493–507.
Moreno, A., Giralt, S., Valero-Garcés, B.L., Sáez, A., Bao, R., Prego, R., Pueyo, J.J., González-Sampériz, P., Taberner, C., 2007. A 14 kyr record of the tropical Andes: The Lago Chungará sequence (18°S, northern Chilean Altiplano). Quat. Int. 161, 4–21.
Moreno, A., Santoro, C.M., Latorre, C., 2009. Climate change and human occupation in the northernmost Chilean Altiplano over the last ca. 11500 cal. a BP. J. Quat. Sci. 24, 373–382.
Mortlock, R.A., Fairbanks, R.G., Chiu, T., Rubenstone, J., 2005. $^{230}Th/^{234}U/^{238}U$ and $^{231}Pa/^{235}U$ ages from a single fossil coral fragment by multi-collector magnetic-sector inductively coupled plasma mass spectrometry. Geochim. Cosmochim. Acta 69, 649–657.
Moy, C.M., Seltzer, G.O., Rodbell, D.T., Anderson, D.M., 2002. Variability of El Niño/Southern Oscillation activity at millennial timescales during the Holocene. Nature 420, 162–165.
Nester, P.L., Gayó, E., Latorre, C., Jordan, T.E., Blanco, N., 2007. Perennial stream discharge in the hyperarid Atacama Desert of northern Chile during the latest Pleistocene. Proc. Natl. Acad. Sci. 104, 19724–19729.
Ortlieb, L., 1995. Eventos El Niño y episodios lluviosos en el Desierto de Atacama: El registro de los dos últimos siglos. Bull. Inst. Fr. Études Andin. 24, 519–537 (in Spanish).
Osmond, J.K., May, J.P., Tanner, W.F., 1970. Age of the Cape Kennedy barrier-and-lagoon complex. J. Geophys. Res. 75, 5459–5468.
Pigati, J.S., Rech, J.A., Quade, J., Bright, J., 2014. Desert wetlands in the geologic record. Earth Sci. Rev. 13, 67–81.
Placzek, C., Quade, J., Patchett, P.J., 2006. Geochronology and stratigraphy of Late Pleistocene lake cycles on the Southern Bolivian Altiplano: implications for causes of tropical climate change. Geol. Soc. Am. Bull. 118, 515–532.
Placzek, C., Quade, J., Betancourt, J.L., Patchett, P.J., Rech, J.A., Latorre, C., Matmon, A., Holmgren, C., English, N.B., 2009. Climate in the dry central Andes over geologic, millennial, and interannual timescales. Ann. Mo. Bot. Gard. 96, 386–397.
Quade, J., Rech, J.A., Betancourt, J.L., Latorre, C., Quade, B., Rylander, K.A., Fisher, T., 2008. Paleowetlands and regional climate change in the central Atacama Desert, northern Chile. Quat. Res. 69, 343–360.
Rech, J., Quade, J., Betancourt, J.L., 2002. Late Quaternary paleohydrology of the central Atacama Desert (22–24°S), Chile. Geol. Soc. Am. Bull. 114, 334–348.
Rech, J.A., Pigati, J.S., Quade, J., Betancourt, J.L., 2003. Re-evaluation of mid-Holocene deposits at Quebrada Puripica, northern Chile. Palaeogeogr. Palaeoclimatol. Palaeoecol. 194, 207–222.
Sáez, A., Cabrera, L., Jensen, A., Chong, G., 1999. Late Neogene lacustrine record and palaeogeography in the Quillagua-Llamara basin, Central Andean fore-arc (northern Chile). Palaeogeogr. Palaeoclimatol. Palaeoecol. 151, 5–37.
Sáez, A., Valero-Garcés, B.L., Moreno, A., Bao, R., Pueyo, J.J., González-Sampériz, P., Giralt, S., Taberner, C., Herrera, C., Gibert, R.O., 2007. Lacustrine sedimentation in active volcanic settings: the Late Quaternary depositional evolution of Lake Chungará (northern Chile). Sedimentology 54, 1191–1222.
Sáez, A., Cabrera, L., Garcés, M., Bogaard, P., Jensen, A., Gimeno, D., 2012. The stratigraphic record of changing hyperaridity in the Atacama desert over the last 10 Ma. Earth Planet. Sci. Lett. 355, 32–38.
Santoro, C.M., Latorre, C., Salas, C., Osorio, D., Ugalde, P., Jackson, D., Gayó, E.M., 2011. Ocupación Humana pleistocénica en el Desierto de Atacama. Primeros resultados de la aplicación de un modelo predictivo interdisciplinario. Chungará 43, 353–366 (in Spanish).
Thomas, J.C., Geisler, D., 1982. Peuplements benthiques à cyanophycees du Salin-de-Giraud. Géol. Mediterr. 9, 391–412.
Thompson, L.G., Davis, M.E., Mosley-Thompson, E., Sowers, T.A., Henderson, K.A., Zagorodnov, V.S., Lin, P.-N., Mikhalenko, V.N., Campen, R.K., Bolzan, J.F., Cole-Dai, J., Francou, B., 1998. A 25,000-year tropical climate history from Bolivian ice cores. Science 282, 1858–1864.
Valero-Garcés, B.L., Delgado-Huertas, A., Navas, A., Edwards, L., Schwalb, A., Ratto, N., 2003. Patterns of regional hydrological variability in central southern Altiplano (18°S-26°S) lakes during the last 500 years. Palaeogeogr. Palaeoclimatol. Palaeoecol. 194, 319–338.
Vargas, G., Ortlieb, L., Rutllant, J., 2000. Aluviones históricos en Antofagasta y su relación con eventos El Niño/Oscilación del Sur. Rev. Geol. Chile 27, 157–176.
Vargas, G., Rutllant, J., Orlieb, L., 2006. ENSO tropical-extratropical climate teleconnections and mechanisms for Holocene debris flows along hyperarid coast of western South America (17°–24° S). Earth Planet. Sci. Lett. 249, 467–483.
Vuille, M., Ammann, C.M., 1997. Regional snowfall patterns in the high, arid andes. Clim. Change 36, 413–423.
Vuille, M., Keimig, F., 2004. Interannual variability of summertime convective cloudiness and precipitation in the central Andes derived from ISCCP-B3 data. J. Clim. 17, 3334–3348.
Zolá, R.P., Bengtsson, L., 2006. Long-term and extreme water level variations of the shallow Lake Poopó, Bolivia. 2006. Hydrol. Sci. J. 51, 98–114.